Article type: Full Paper

Long-term Tissue Culture of Adult Brain and Spleen Slices on Nanostructured Scaffolds

Sonja Kallendrusch[+], Felicitas Merz[+], Ingo Bechmann, Stefan G. Mayr and Mareike Zink

[+]shared authorship

Dr. S. Kallendrusch, Prof. Dr. I. Bechmann

Institute of Anatomy, University of Leipzig, Oststr.25, 04317 Leipzig, Germany

Dr. F. Merz

Institute of Anatomy, University of Leipzig, Oststr.25, 04317 Leipzig, Germany, now at GSI Helmholtz Centre for Heavy Ion Research, Planckstr. 1, 64291 Darmstadt

Prof. Dr. S.G. Mayr

Leibniz Institute for Surface Modification (IOM), Permoser Str. 15, 04318 Leipzig, Germany and Division of Surface Physics, Department of Physics and Earth Sciences, University of Leipzig, Leipzig, Germany

Dr. M. Zink

Soft Matter Physics Division, Institute for Experimental Physics 1, University of Leipzig, Linnéstr. 5, 04103 Leipzig, Germany

Corresponding author E-mail: zink@physik.uni-leipzig.de

Keywords: culture scaffolds, adult tissue culture, nanotubes, brain tissue, spleen tissue

Abstract

Long-term tissue culture of adult mammalian organs is a highly promising approach to bridge the gap between single cell cultures and animal experiments, and bears the potential to reduce *in vivo* studies. Novel biomimetic materials open up new possibilities to maintain the complex tissue structure *in vitro*; however, survival times of adult tissues *ex vivo* are still limited to a few days with established state-of-the-art techniques. Here we demonstrate that TiO_2 nanotube scaffolds with specific tissue-tailored characteristics can serve as superior substrates for long-term adult brain and spleen tissue culture. High viability of the explants for at least two weeks was achieved and compared to tissues cultured on standard PTFE membranes. Histological and immunohistochemical staining and live imaging were used to investigate tissue condition after 5 and 14 days *in vitro*, while environmental scanning electron microscopy qualified the interaction with the underlying scaffold. In contrast to tissues cultured on PTFE membranes, enhanced tissue morphology was detected in spleen slices, as well as minor cell death in neuronal tissue, both cultured on nanotube scaffolds. This novel biomimetic tissue model will prove to be useful to address fundamental biological and medical questions from tissue regeneration up to tumor progression and therapeutic approaches.

1. Introduction

Two incidents in recent history have dramatically demonstrated the urgent need for innovative methods in clinical and basic research for more sensitive test models before pursuing first-in-man-studies: A recent clinical trial of BIA 10-2474, a FAAH (Fatty acid amide hydrolase) inhibitor in France, resulted in one fatality and six people needing intensive care.[1] Within another clinical trial known as ‘London tragedy` all volunteers suffered from severe shock syndromes even though animal tests with primates had not indicated any side effects.[2] In fact, since the screening process to validate novel therapeutics is long and often not efficient, as seen in the clinical trials mentioned above, new methods that contain more complex tissue settings *ex vivo* are needed to determine mechanisms of drug actions prior to time intense animal testing.

Organotypic slice cultures are suitable to fill the gap between cultured cells and *in vivo* studies as they add the complex crosstalk of different cell types.[3–7] However, for neuronal tissues this method is up to now only applicable to embryonic or newborn tissue due to its regenerative capacity and plasticity. Therefore, it is often used in developmental studies.[7,8] For example; brain tissue of 3 to 5 days old rodents can be kept in culture for months, whereas brain slices of adult mice, which are fully differentiated, are only used in acute experiments for some hours because neuronal activity decreases significantly afterwards.[9,10] However, many biological reactions or mechanisms, as well as the development of drugs, e.g. for neuroactivation, can only be tested on fully differentiated adult tissues which display different cellular and extracellular characteristics compared to young or embryonic tissue or even cell cultures.[11,12]

The basic tissue culture experiments performed in the 1990s implied the need to cultivate the tissue slices on a liquid-air interface.[4] In addition, more recent studies found that good adhesion of the tissue to the underlying scaffold is an important prerequisite for maintaining organotypic tissue culture.[13–15] The surface structure of the scaffold material determines

physical properties such as hydrophilicity as well as surface charges and energy. Those properties in turn trigger protein adsorption important for cell adhesion.[16] Surface morphology and roughness on nanometer length scale also have great influence on cell attachment.[17] Especially the length scale of the topography modulation plays a crucial role on integrin clustering during cell adhesion, since integrin receptors of ~23 nm width can sense roughness gradients down to 8 nm.[18] Moreover, spacing of the amino acid sequence arginine-glycine-aspartic (RGD), specific for integrin receptor binding on the cell surface must be smaller than ~70 nm to form focal adhesions.[19] Thus, scaffolds that provide adhesion of RGD peptides of the required density and length scale are the first step in cell adhesion. However, it is still a matter of debate whether good adhesion of single cells is an important scaffold feature for tissue and organ culture, since cell migration out of the tissue and disruption of the organotypic structure could be promoted.[20] Alternatively, attachment of extracellular matrix (ECM) molecules to the scaffold might promote complete tissue adhesion for long-term organotypic culture which could explain why tissues from different origins behave differently *ex vivo* on scaffolds with nanostructured topography.[20]

To this end, nanodevices that mimic the nanotopography of the ECM offer new strategies for maintaining or even engineer tissues *in vitro*.[21] These devices can be built from metals or any other biocompatible materials, often in combination with ECM components. A new approach employs tunable TiO_2 nanotube scaffolds which comprise parallel aligned TiO_2 tubes of diameters ranging from ~10-150 nm diameter (for an overview see [22]).

Here we demonstrate that brain and spleen tissues from adult mice can be long-term cultured organotypically on nanostructured TiO_2 scaffolds with tissue-specific tailored nanogeometry. In addition to tuning the structure of the affordable and reusable TiO_2 nanotube scaffolds, we use morphological analyses, live confocal microscopy and immunohistochemical stainings to show that the tissue structure is preserved for two weeks. Differences of tissue adhesion on nanotube scaffolds compared to commonly used PTFE

membranes was investigated by environmental scanning electron microscopy (ESEM) demonstrating the importance of good tissue-scaffold interconnection. Thus, scaffolds with tissue-adapted geometry at the nanoscale offer the possibility to maintain adult tissue cultures *in vitro* and address fundamental biological questions, as well as to study new therapeutics and immunological reactions.

2. Results

2.1 Cultivating adult organotypic tissue slices on different scaffolds

In this study, we investigated long-term cultures of adult tissue slices (rodent hippocampus and spleen) on TiO_2 nanotube scaffolds and compared tissue integrity and cell survival with control experiments on widely used PTFE membrane inserts (information on porous membranes for tissue culture can be found in Ref. [23]). TiO_2 scaffolds were synthesized by electrochemical anodization of titanium plates in ammonium fluoride containing solution as described in the methods section. While one anodization step usually results in freestanding (FS) nanotube scaffolds with rough surfaces (**Figure 1A**), two and more can be employed for smooth and nanoporous (NP) nanotube scaffolds (Figure 1B). Surface analysis by scanning electron microscopy (SEM) and atomic force microscopy (AFM) revealed that the NP structure was composed of nanotube diameters d=(100.0±12.0) nm, wall thickness t=(8.0±1.5) nm and a root-mean-square (RMS) roughness σ= 63 nm with a surface modulations length of λ > 150 nm.[20] The roughness arises from variations of individual tube heights h_i around the average surface plane, as measured by atomic force microscopy (AFM) and characterized – normal to the surface – by the standard deviation $\sigma = \sqrt{\langle h_i^2 \rangle - \langle h_i \rangle^2}$, and – in plane - by the characteristic length scale of the modulations, λ, which were calculated as described previously.[20,24] In contrast, FS nanotube scaffolds

showed a diameter of d=(57.6±1.2) nm, wall thickness t=(6.2±1.1) nm, and a RMS roughness of σ= (137.0±5.5) nm with surface modulations λ=(1.9±0.2) µm.

For control experiments commercially available PTFE membrane inserts were used as recommended by the manufacturer. SEM imaging was employed to visualize the surface structure (Figure 1C).

For tissue slice cultures, the reusable nanotube scaffolds were sterilized in 70 % ethanol for at least one hour and then transferred to HBSS buffer for equilibration. In the meantime, tissue slices were prepared and placed onto the nanotube scaffolds (**Figure 1D**), as well as the PTFE membranes. Culture medium was filled up just below the scaffold level that the air-liquid-interface principle as described by Stoppini *et al.* was met. Here the nanotube scaffolds, as well as the PTFE membrane have to get in contact with the medium, while the tissue remains exposed to air. Due to the super-hydrophilic character of the scaffold surface,[20] a thin film of medium entirely wets the entire scaffold surface (Figure 1D, E), with continuous exchange with the bulk liquid reservoir by diffusion, thus rendering perfusion systems obsolete. We would like to point out that culture medium cannot diffuse through the nanotubes similarly to medium diffusion through the PTFE membrane since the nanotube scaffold is composed of three layers: On top and on the bottom a few micrometer-thick nanotube layer is formed during electrochemical anodization, while a bulk titanium core stabilizes the scaffold which makes it easy to handle during culture and cleaning. Thus, medium diffuses from the scaffold-side to the top where the tissue is placed.

2.2 Tissue morphology on nanotube scaffolds and PTFE membrane

After cultivating adult murine brain and spleen slices for 5 and 14 days, we first analyzed tissue morphology with classic HE staining and evaluated appearance of nuclei (**Figure 2A**: A-F for brain and G-L for spleen tissue). At higher magnifications, some condensed nuclei indicating cell death are visible in all brain and spleen slices, whereas this observation is

more pronounced in the latter (Figure 2B: A-C for brain and G-L for spleen tissue). For brain slices, we focused on the *dentate gyrus* (dg) region of the hippocampus which is established to play a crucial role in memory formation, but also harbors neuronal stem cells. We found that the general tissue structure is better preserved on both nanotube structures (freestanding and nanoporous, Figure 2, left (NP) and middle (FS) panel) compared to PTFE membranes (right panel). In fact, the neuronal band of the granular cell layer in the dg (Figure 2 A-C and G-I) is more compact and the structure of the hippocampal formation is superior preserved on nanotube scaffolds. The pyramidal neurons of the *cornu ammonis* region 3 of the hippocampal formation are again less hemalaun positive than in brain tissues of nanotube scaffolds, indicating a low DNA/RNA content (Figure 2A: A-F). In Figure 2B, toluidine blue staining is used to visualize DNA and the endoplasmatic reticulum, illustrating the granule cell layer in more detail, where intact nuclei and preservation of ER are visible. Brain tissue on NP scaffolds maintain the granule characteristic of the *dentate gyrus* layer, demonstrating conserved dense cell nuclei. At 14 dic a distinct change of the pyramidal cells, situated between the dg and the *cornu ammonis* region (CA3), as well as a cell loss in the *stratum moleculare,* can be determined on tissue cultured on PTFE membrane.

Examination of vertical sections through brain tissue additionally confines optimal tissue integrity of NP scaffolds by demonstrating equal cellular distribution throughout the complete vertical section (Figure 2B). Cultures on FS scaffolds, as well as the PTFE membranes, exhibit a cellular gradient towards the tissue surface (upper side). As hemalaun stain is basophil, thus marking the acidic structures in blue, the surface of the PTFE membrane clearly shows an acidic tissue environment.

In spleen slices, preservation of typical structures like capsule and follicles (“f” in Figure 2A: G-L, Figure 2B: G-L) was examined. Morphological integrity is again better preserved on the NP and FS scaffolds than on PTFE membranes. After already 5 dic tissue alterations are clearly distinct, while adult spleen tissue of mice maintained its structure up to 14 dic on

nanotube scaffolds (Figure 2A: G-L). The central artery is maintained in all tissues; however, in tissue cultivated on PTFE membranes the connective tissue has clearly expanded and vessels are less conserved. The follicular structure is best maintained on FS scaffolds; here the typically inconspicuous follicles of the mouse spleen are seen. The periarteriolar lymphoid sheaths (macrophage-, T-cell- rich), as well as a coronal zone (small to medium lymphocytes) can be determined. The *germinal centers* (G) are not visible, which can be explained by missing immunological stimuli (Figure 2A: G-L, 2b G-L). We did not extract spleen capsule prior to tissue culture and observed good capsule preservation in spleen tissue cultured on FS scaffolds. PTFE membranes could not maintain spleen capsule as tissue integrity was lost completely. NP scaffolds, however, again preserved the capsule of the spleen tissue, but the capsule became dense and demonstrated less ECM compared to cultures on their FS counterparts (Figure 2B).

2.3 Confocal live imaging of living and dead cells

To analyze structure and cell survival of adult murine tissues of complete coronal brain slice and spleen slice cultures in more detail, we performed confocal live imaging at two times (5 and 14 dic). To this end, we visualized cell damage and dead cells by employing Propidium Iodide (PI, red). The background staining of PI also allowed observation of tissue integrity that was enhanced in tissues on nanotube scaffolds in contrast to cultures on PTFE membranes (**Figure 3**). Only few PI positive nuclei could be detected in brain tissue cultures with NP nanotube scaffolds, which appeared only in the hippocampal formation and not in the cortex region. In contrast, PI positive nuclei were visualized in the cortex and hippocampal formation of brain tissue cultures on FS nanotube scaffolds. Brain tissue of both scaffolds did not show obvious changes comparing 5 dic and 14 dic samples (Figure 3 A, B, D, E). However, brain tissue on PTFE membranes showed many PI positive cells in

the cortical, as well as in the hippocampal region. Reduced background staining may also indicate loss of tissue integrity, due to less fluorophore retain by the tissue (Figure 3 C, F). Adult murine spleen tissue integrity was also conserved after 5 and 14 dic, when cultured on nanotube scaffolds (Figure 3 G, H). FS scaffolds maintained spleen tissue even better since less PI positive cells and enhanced tissue integrity could be observed compared to NP scaffolds or PTFE membranes. Spleen tissue cultured on PTFE membranes showed high amounts of PI positive nuclei on 5 as well as 14 dic (Figure 3 I). PI uptake was mostly restricted to follicles, which contain the B- and T-lymphocytes in contrast to splenic parenchymal tissue.

Nuclear counterstaining with Hoechst 33342 in cryosections of fixed tissue allowed to evaluate intact cell nuclei in relation to damaged or dead cells (PI positive) (Figure 3 B). PTFE membranes showed enhanced cell damage in cultured brain tissue, while NP nanotube scaffolds maintained best cell viability of cultured brain tissue.

2.4 Analysis of apoptosis and general cell death on different culture scaffolds

Neurons as the functional cells in the brain are sensitive to influences from environmental changes, e.g. caused by culturing conditions. In order to investigate neuronal preservation as well as general cell death, we used immunofluorescent staining for NeuN, a neuronal marker (green, **Figure 4** A-C), and cleaved Caspase 3 (Cas3), an apoptosis marker (green, Figure 4 D-O), in combination with nuclear counterstaining (Hoechst, blue). After 5 dic, neurons were present in all slices independent of the scaffold on which they were kept. However, the granular cell layer exhibits less NeuN expression on PTFE membranes (Figure 4 C) in contrast to slices cultivated on nanotube scaffolds (Figure 4 A-B).

In brain slice cultures, almost no Cas3 positive cells became visible on nanotube scaffolds, whereas brain tissue on NP nanotubes even showed less Cas3 positive cells compared to FS ones (Figure 4 D, E). Brain tissue cultured on PTFE membranes demonstrated a higher

number of apoptotic cells (Figure 4 F). Quantitatively, the apoptosis rate on PTFE membranes is approximately three times higher compared to both nanotube scaffolds.

In spleen slice cultures, the apoptosis rate after 5 and 14 dic is generally higher compared to PTFE membranes on which the overall cell density, characterized by blue nuclear staining, is considerably lower (Figure 4 J-O).

2.5 Analysis of tissue adhesion to nanotube scaffolds and PTFE membranes

As already stated by Hofmann, good adhesion of the tissue to the underlying scaffold is important for successful organotypic culture.[25] To this end, we performed environmental scanning electron microscopy (ESEM) imaging of cultured tissues to the different culture scaffolds to investigate the scaffold-tissue interface. After 5 days in culture, tissue slices were fixed on top of their scaffolds and analyzed by ESEM. **Figure 5** illustrates the adhesion of brain slices onto their scaffolds with a focus on the edges and the connection with the different surfaces. On nanotube scaffolds (A and B: freestanding, B and C: nanoporous), the tissue seems to form a steady, continuous adhesion with the scaffold along the entire tissue edge. There is no visible gap between the tissue and the nanotube material. In contrast, on the PTFE membrane the tissue does not connect to the scaffold and only forms punctuate connections (Figure 5E, F). The tissue-scaffold interaction becomes even more obvious under higher magnifications when the smooth adhesion along the entire tissue edge is visible on the nanotubes (Figure 5G, H), whereas a punctuate outgrowth on a PTFE membrane becomes present (Figure 5I, J). It is worth mentioning that the tissue cultured on the PTFE membranes can easily be peeled of the surface, while for the nanotube scaffolds the adhesion is so strong, that it can hardly be detached.

To investigate the origin of strong tissue adhesion to the nanotube scaffolds in more detail, we soaked FS nanotube scaffolds, as well as PTFE membranes in a diluted solution of fluorescently labelled laminin (see Supporting Information, **Figure S1**). Laminin is a major

component of the brain ECM and contains the binding site for specific adhesion of cells. Here we found that almost no laminin adsorption occurred on PTFE, while the entire nanotube surface was covered with laminin. For comparison we also checked for protein adsorption on unstructured TiO_2 surfaces. Here also no laminin adsorption was seen which might be the reason why the tissue can also not adhere to unstructured TiO_2 as seen in earlier experiments (not shown).

Finally we also cultured the brain and spleen slices on nanotube scaffolds with other nanotube geometries in terms of tube diameter, wall thickness and surface roughness. We found that tissue preservation was not maintained on any of these scaffolds. Thus, the presented NP nanotube scaffolds represent ideal surface topographies for adult hippocampal slice culture with a very low apoptosis rate even after 14 days. For spleen culture the FS nanotube structure is favored. However, here the nanotopography might even get more optimized to further reduce apoptosis in long-term culture. The culture conditions for spleen slices can be further optimized by using specialized media for lymphatic tissues. Nevertheless, the employed nanotube scaffolds maintain the tissue structure of brain and spleen slices much better compared to standard PTFE membranes.

3. Discussion

Organotypic culture of adult tissues is still an unsolved challenge since cell survival, especially in the case of sensitive neurons, and integrity of the entire tissue architecture can only be maintained for a few days.[26] However, new culture models of fully differentiated tissue structures are demanding to study neurodegenerative diseases, including e.g. Alzheimer, and drug screening.[23]

Over the past years intensive research in the field of nanotechnology paved the way for new culture models on the basis of nanostructured scaffolds. In contrast to flat surfaces, the nanotopography can be tuned to match the length scales of focal adhesions to promote cell

adhesion, motility and even trigger stem cell differentiation [27,28] and fate [17,29] (for an overview see e.g. [30]). In our study, adult rodent hippocampal tissue and spleen slices were cultured on TiO_2 nanotube scaffolds and examined after 5 and 14 days. We found that the organotypic structure of rodent brain and spleen slices strongly depend on the nanogeometry of the underlying nanotube scaffolds. While nanoporous nanotubes with tube diameters of 100.0±12.0 nm and roughness of 63 nm are ideal for long-term culture of adult rodent brain slices, freestanding nanotube scaffolds with smaller diameters of 57.6±1.2 nm and rougher surfaces of 137.0±5.5 nm support cell survival of adult rodent spleen slices. Larger or smaller nanotube diameters result in cell dissolution.

We studied the hippocampal region with its dense neuronal structure in horizontal and vertical dimensions and observed good tissue preservation in brain tissue cultures cultivated on nanotube scaffolds in contrast to brain tissue cultured on PTFE membranes. Nanoporous nanotubes even conserved the tissue integrity and showed improved neuronal NeuN expression than on the freestanding nanotube geometry. It was previously demonstrated that NeuN is a marker for postmitotic neurons and that injuries such as ischemia or axonal injury may lead to reduced or even loss of NeuN protein expression.[31–35] In our experiments, neurons of the granular cell layer lost their NeuN expression completely on PTFE membranes indicating neuronal deafferentation or damage, whereas more neurons remained NeuN positive on nanotube scaffolds.

Even though adult brain tissue cultures bear great potential to study neuroplasticity and neuronal dysfunctions related to aging *in vitro*, up to now cell survival times of more than a few days is hardly reached. Mewes *et al.* compared organotypic brain slice cultures of adult transgenic P301S postnatal mice with adult animals.[9] They observed that vitality of adult slice cultures significantly decreased upon cultivation of 2 weeks, while the postnatal cultures were still at a high vitality level. Kim *et al.* demonstrated a prolonged neuronal survival for adult OHSC in serum-free conditions.[36] However, serum-free cultures reflect *in*

vivo conditions to a much smaller extent since possible changes in the ECM and, e.g. altered drug and gene regulation, need to be considered. Another approach to prolong adult hippocampal slice cultures is manipulating the culture media.[37] Here electrophysiology was employed to demonstrate neuronal survival, while after 6 days a decline in neuronal activity was observed. Humpel also obtained that survival of neurons in adult murine brain slices can hardly be maintained for 2 weeks even in the presence of special growth factors.[38]

In contrast to brain tissue, culture of spleen slices seems to be a neglected method in studies investigating pathogenesis of infectious agents, since spleen tissue cultures represent a model for a wide range of immunological questions. In our study, tissue integrity and cell death (PI, Cas3) were investigated in vertical and horizontal dimension in adult spleen cultures. Here, spleen tissue obtained its full architecture when cultivated on freestanding nanotube scaffolds, and apoptosis and cellular damage of tissue cultured on nanotubes were less pronounced compared to tissue cultured on PTFE membranes. Interestingly, good long-term culture conditions for hippocampus and spleen were obtained on different nanotube geometries as mentioned above.

Our experiments showed that brain and spleen tissue adhesion to the underlying scaffold is a major determinant of tissue preservation. Inadequate nanotube geometries suppress adhesion and likely results in tissue dissolution. Interestingly, the ideal scaffold surface structure is tissue-type dependent. Thus, we do not consider possible variations in hydrophilicity or sufficient nutrient by diffusion supply a possible reason for long-term tissue preservation since spleen and brain tissue cultures contained the same culture media and for both employed nanotube diameters the surfaces exhibit a super-wetting behavior.[20,39]

To corroborate our observation that tissue adhesion is an important factor for long-term culture as already proposed by Hofmann,[25] we studied the tissue-nanotube interface with environmental scanning electron microscopy. We obtained that brain and spleen tissue slices adhere to the nanotubes along the entire tissue-scaffold interface and formed a

continuous adhesion border. In contrast, on the PTFE membranes only few contact points could be observed, while cell migration out of the tissue to the surface of the membrane became evident.

The reasons why cells and tissues show an improved adhesion on nanostructured surfaces is still a matter of debate. Recently, we demonstrated the effect of protein adsorption from serum in culture medium on TiO_2 nanotubes.[40] In this study albumin and fibronectin in contact with the scaffold adsorb on and inside the nanotubes. Fibronectin adsorption strongly enhances cell adhesion since it can specifically bind to integrin receptors on the cell surface. However, fibronectin adsorption cannot explain why cell and tissue adhesion selectively depend on the nanotube diameter. For rodent brain slices one of the major ECM molecules is laminin.[23] This glycoprotein shows improved adsorption on the nanotubes compared to untreated TiO_2 surfaces and PTFE membranes on which almost no adhesion could be observed (see Supporting Information). Nevertheless, as shown by Scopelliti *et al.*, the nanotopography greatly influences protein adsorption and even small variations in nanoscale roughness can induce significant changes in protein binding affinity.[41] In contrast to the ECM of brain tissues, a narrow net of fibrillary collagen type, I, II, IV and reticular fibers of collagen type III construct the ECM of the spleen together with smaller portions of laminin and other proteins.[42] Depending on the tissue type, collagen molecules assemble into complex structures with diameters in the range of 30 to 500 nm.[43] Since hippocampal and spleen tissues exhibit different ECM compositions, it is not surprising that each tissue needs an adapted nanotube structure that matches the nanostructure of the ECM. To this end, even small nanotube variations hinder tissue attachment. It also has to be taken into account that not only the density of adhesion sites of ECM molecules is important for cell adhesion, but also the spacing between the adhesive spots which are usually composed of RGD clusters.[17] The formation of such clusters and the spacing can directly be tuned by the underlying nanotopography of the scaffold.

Our preliminary data on adult human tonsil tissue on the same nanotube scaffolds as employed for brain and spleen slices show that the employed nanotube geometries do not provide better culture conditions than PTFE membranes (see Supporting Information, **Figure S2**), which is not surprising since the architecture and composition of the ECM and cells within human tonsils differs significantly from rodent brain and spleen. However, current investigations focus on improved tissue preservation as a function of nanotube geometry for various tissue types.

In summary, tissue culture of adult rodent brain and spleen slices of at least 14 days on TiO_2 nanotube scaffolds is possible when the optimal nanotube geometry is employed. In contrast to culture systems such as 3D embedding gels or bioreactors,[26] tissue culture on the nanotube scaffolds is easy and also perfusion systems for better medium supply are not necessary due to the hydrophilicity of the surface and the continuous intrinsic renewal of the medium film from the liquid reservoir under the scaffold. Besides, scaffolds can be cleaned (protocol see Supporting Information), sterilized and reused several times. Future work will focus on the interaction of ECM molecules with nanotube scaffolds by investigating protein adsorption and tissue attachment with STED microscopy and ESEM for a better understanding how the nanogeometry influences organotypic structure preservation.

4. Conclusion

Up to now hardly any culture system allows culture times of adult mammalian tissues of more than a few days. Thus, our novel biotechnological concept of employing TiO_2 nanotube scaffolds offers new perspectives in adult organotypic tissue culture, enabling neurobiological approaches in brain research as well as immunological reactions *in vitro* with the application of spleen tissue. Additionally, drug testing prior to clinical trials can help to prevent adverse events in humans as seen e.g. for the “London tragedy”. Even though blood circulation is missing, the potential of organotypic culture was already shown by Nitsch

et al. who employed human neuronal slice cultures to demonstrate neurotoxic effects of trimerized TRAIL without the need of clinical tests.[44] Adaptation of the presented nanotube geometry to allow for long-term culture of human tissues such as tonsils (preliminary data see Supporting Information) and tumors even bears the potential to narrow the gap between fundamental research and clinical settings. [5,6,45]

5. Experimental Section

Nanotube Scaffold Preparation

Nanotube scaffolds were synthesized by electrochemical anodization. First, the titanium foil (Advent Research LTD; 99.6 %; size 3 cm x 3 cm, thickness 0.1 mm) which acts as an anode was cleaned in an ultrasound bath with distilled water and isopropyl alcohol for 10 min each. Afterwards the foil was dried in a nitrogen steam. For anodization an electrolyte solution of ethylene glycol (Merck KGaA, Darmstadt, Germany) was prepared containing 2 vol. % distilled water and 0.3 wt. % ammonium fluoride (Sigma-Aldrich, Steinheim, Germany). For anodization the electrolyte solution, the titanium foil (anode) and a platinum mesh (cathode; Advent Research LTD; 99.9 %; 52 mesh per inch; size 2.5 cm x 2.5 cm) were placed in a plastic vessel with the electrodes connected to an external DC power supply.

To obtain free-standing (FS) nanotube scaffold with rough surface topography and smaller nanotube diameters, a voltage of 40 V was applied for 60 min. For the nanoporous (NP) nanotube scaffold with smoother surface and larger diameters, two anodization steps were necessary with the first anodization at 60 V for 40 min and 80 V for 60 min. In between the titanium was cleaned in water with an ultrasound bath for 15 min. Afterwards all samples were rinsed with ethylene glycol and dried on air at 43 °C overnight.

Surface characterization of nanotube scaffolds

Surface topography of the nanotube scaffolds was characterized by scanning electron microscopy (SEM) and atomic force microscopy (AFM). For SEM imaging a Zeiss ULTRA 55 Field Emission Scanning Electron Microscope (Germany) was employed with an acceleration voltage of 15 kV and an in-lens secondary electron detector. Images were then recorded to evaluate the nanotube diameter in terms of the internal tube cross-sections, as

well as wall thickness. Errors were estimated from the corresponding standard deviations of several tens of analyzed nanotubes.

Surface roughness of the nanotube scaffolds was assessed as described before.[20]

Organotypic tissue cultures

Animals were kept according to the national regulations of animal welfare. Adult wildtype C57black6 mice (8 weeks to 6 months old) were sacrificed using Isoflurane anesthesia followed by cervial dislocation as approved by the local authorities (T09/14, Landesdirektion Sachsen, Germany). Brains and spleens were quickly removed under sterile conditions and transferred to 4°C minimal essential medium (MEM; Gibco BRL Life Technologies, Eggenstein, Germany) containing 1 % (v/v) glutamine (Gibco). A sliding vibratome (Leica VT 1200 S, Leica Microsystems AG, Wetzlar, Germany) was used to horizontally cut the tissues in 350 µm-thick slices. The slices were then placed on nanotube scaffolds or the standard cell culture inserts (PTFE, MERCK Millipore) by using a glass pipette with a wide opening.

The nanotube scaffolds of about 2x2 cm size were placed onto an autoclaved ring, placed in 6-well culture dishes (Falcon, BD Biosciences Discovery Labware, Bedford, MA) containing culture medium (50 % (v/v) MEM, 25% (v/v) Hanks' balanced salt solution (HBSS, Gibco), 25 % (v/v) normal horse serum (NHS, Gibco), 2 % (v/v) glutamine, 1 % glucose (45 % stock solution B.Braun, Melsungen, Germany), 0.1 mg/ml streptomycin (Sigma-Aldrich, Deisenhofen, Germany), 100 µg/ml penicillin (Sigma-Aldrich)) (Figure 1).

For tissue culture on PTFE membranes, 1 ml culture medium per well is recommended by the manufacturer, for nanotube scaffolds, we used 2-3 ml due to a different height of the substructure, the scaffolds were just in contact with the medium, while the tissue was not covered with liquid (liquid- air interface- technique). The cultures were kept at 37 °C in a

fully-humidified atmosphere with 5 % (v/v) CO_2 up to 14 days. The culture medium was changed every other day.

Staining of tissue cultures for live confocal imaging

Brain and spleen slice cultures on nanotube substrates or standard membranes were cultivated for 5 or 14 days as described above. Subsequently, Propidium Iodide (PI, red) for dying cells was added to the culture medium two hours before imaging. Medium was changed to remove excess dye, and Z-stacks were acquired with an Olympus FV1000 confocal microscope equipped with a climate chamber to keep a constant temperature of 36 °C, 60 % humidity and 5 % CO_2 concentration at 10x magnification with a long-distance objective and constant laser and exposure intensities. Afterwards, slices were fixated for further analyses.

Embedding and staining procedure

After 5 or 14 days in culture (dic), slices were fixed with 4 % paraformaldehyde for 4 h and washed with PBS. Standard paraffin embedding is delicate when tissues need to be embedded horizontally. Therefore, small embedding cassettes and filter paper (Medite GmbH, Germany) were used to maintain the tissue flat and straight. Afterwards, the tissues were cut into 7 µm sections, placed on glass slides and dried. For morphological analysis, sections were dewaxed in a decreasing xylene/alcohol series, rehydrated and stained with hematoxylin/eosin (HE). Images were taken with a Zeiss Axioplan 2 (Carl Zeiss AG, Oberkochen, Germany).

For analysis of cellular distribution in slices, cryosections were employed. To this end, slices were fixed as described above, washed in PBS, incubated with an increasing series of sucrose in PBS (10, 20 and 30 %, 12-24 h each), mounted in TissueTek (Sakura Finetek USA Inc.) and frozen at -20 °C. Mounting was either realized flat on a pre-cropped TissueTek

block for horizontal sectioning, or slices were frozen in TissueTek and rotated by 90° before mounting and cutting. We gained cross sections through the slices, showing the area between the surfaces in contrast to the horizontal sections, which allows observation of tissue structure and possible gradient changes towards the tissue surface.

For immunohistochemical stainings, paraffin sections were dewaxed and rehydrated as indicated above. Cryosections were dried and washed in PBS. Afterwards, 10 % normal goat serum in PBS/Triton (0.3 %) was applied as blocking solution for one hour. The following primary antibodies were used and incubated over night at 4 °C: Ki-67 (BD Pharmingen, cat. No. 556003, USA; mouse, 1:200), NeuN (Millipore, cat.-No. MAB377, USA, mouse, 1:200) and Cleaved caspase 3 (Cell Signaling Technology, cat-No. 9661, USA; rabbit, 1:400). For Caspase-3 staining, slides were pre-treated with Citrate buffer at pH 6 at 95 °C in a microwave oven for 10 minutes. After a washing step with PBS, sections were incubated with the secondary antibodies, goat-anti mouse and goat-anti rabbit, conjugated with Alexa Fluor 488 (Invitrogen) and washed again. Hoechst 33342 was used for visualization of nuclei. Sections were covered with DAKO fluorescent mounting medium (DAKO, Hamburg, Germany) for storage. Images were taken and analyzed using a Zeiss LSM 510 confocal microscope (Carl Zeiss AG, Oberkochen, Germany) or an Olympus BX51 (Olympus, Hamburg, Germany).

Quantification of apoptotic cells

Caspase-3-positive cells and total cell nuclei were quantified by counting 6 pictures of at least two independent cultures per condition with the Image J Cell Counter plug-in [46]. One-way ANOVA was applied with Graph Pad Prism 5 (GraphPad Software, Inc., La Jolla, CA, USA), and $p<0.05$ was considered significant.

Tissue and PTFE membrane imaging with environmental scanning electron microscopy (ESEM)

Tissue was cultivated as described below for 5 days, subsequent the cultures were fixed with 4% PFA for 4 h and were washed in PBS prior to ESEM imaging. Samples were examined with a FEI ESEM at 10 kV acceleration voltage under wet mode conditions using a large-field detector (LFD). The scaffold with the tissue on top was clamped onto the holder of a Peltier stage. The stage temperature was constant at 4 °C that a saturated vapor pressure within the chamber was maintained at 500 Pa. ESEM imaging of PTFE filters (pore size 0.4 µm; MERCK Millipore, Darmstadt, Germany), which are routinely used in tissue culture, was performed in high-vacuum mode with an Everhart-Thornley Detector (ETD) and an acceleration voltage of 5 kV.

Supporting Information

Supporting Information is available from the Wiley Online Library or from the author.

Acknowledgements

This work was funded in parts by the BMBF, Projects “EYECULTURE” (FKZ 031A574) and “GBM-hOSC” (FKZ 031A579). The authors acknowledge Astrid Weidt for the laminin adsorption experiments, Constance Hobusch and Angela Ehrich for help with tissue processing. It is also a pleasure to thank Paul Noske, Steven Huth, Marcus Müller, David Poppitz and Alexander Jakob for help with nanotube synthesis as well as (E)SEM and previous AFM measurements, respectively. SK and FM contributed equally to this work.

Literature

[1] N. Moore, *BMJ (Clinical research ed.)* **2016**, *353*, i2727.

[2] D. Eastwood, L. Findlay, S. Poole, C. Bird, M. Wadhwa, M. Moore, C. Burns, R. Thorpe, R. Stebbings, *British journal of pharmacology* **2010**, *161*, 512.

[3] A. de Simoni, L. M. Y. Yu, *Nature protocols* **2006**, *1*, 1439.

[4] L. Stoppini, P. A. Buchs, D. Muller, *Journal of neuroscience methods* **1991**, *37*, 173.

[5] F. Merz, F. Gaunitz, F. Dehghani, C. Renner, J. Meixensberger, A. Gutenberg, A. Giese, K. Schopow, C. Hellwig, M. Schäfer, M. Bauer, H. Stöcker, G. Taucher-Scholz, M. Durante, I. Bechmann, *Neuro-oncology* **2013**, *15*, 670.

[6] M. M. Gerlach, F. Merz, G. Wichmann, C. Kubick, C. Wittekind, F. Lordick, A. Dietz, I. Bechmann, *British journal of cancer* **2014**, *110*, 479.

[7] K. Letinic, R. Zoncu, P. Rakic, *Nature* **2002**, *417*, 645.

[8] J. A. Del Río, B. Heimrich, V. Borrell, E. Förster, A. Drakew, S. Alcántara, K. Nakajima, T. Miyata, M. Ogawa, K. Mikoshiba, P. Derer, M. Frotscher, E. Soriano, *Nature* **1997**, *385*, 70.

[9] A. Mewes, H. Franke, D. Singer, *PloS one* **2012**, *7*, e45017.

[10] T. Su, B. Paradiso, Y.-S. Long, W.-P. Liao, M. Simonato, *Brain research* **2011**, *1385*, 68.

[11] L. E. Sundstrom, *EMBO reports* **2007**, *8 Spec No*, S40-3.

[12] B. Drexler, H. Hentschke, B. Antkowiak, C. Grasshoff, *Current medicinal chemistry* **2010**, *17*, 4538.

[13] R. V. Mundra, X. Wu, J. Sauer, J. S. Dordick, R. S. Kane, *Current opinion in biotechnology* **2014**, *28*, 25.

[14] A. Díaz Lantada, B. Pareja Sánchez, C. Gómez Murillo, J. Urbieta Sotillo, *Expert review of medical devices* **2013**, *10*, 629.

[15] S. Bajpai, N. Y. Kim, C. A. Reinhart-King, *IJMS* **2011**, *12*, 8596.

[16] M. S. Lord, M. Foss, F. Besenbacher, *Nano Today* **2010**, *5*, 66.

[17] M. J. Dalby, N. Gadegaard, R. O. C. Oreffo, *Nature materials* **2014**, *13*, 558.

[18] L. E. McNamara, T. Sjöström, K. Seunarine, R. D. Meek, B. Su, M. J. Dalby, *Journal of tissue engineering* **2014**, *5*, 2041731414536177.

[19] C. Selhuber-Unkel, T. Erdmann, M. López-García, H. Kessler, U. S. Schwarz, J. P. Spatz, *Biophysical journal* **2010**, *98*, 543.

[20] V. Dallacasagrande, M. Zink, S. Huth, A. Jakob, M. Müller, A. Reichenbach, J. A. Käs, S. G. Mayr, *Advanced materials (Deerfield Beach, Fla.)* **2012**, *24*, 2399.

[21] T. Dvir, B. P. Timko, D. S. Kohane, R. Langer, *Nature nanotechnology* **2011**, *6*, 13.

[22] P. Roy, S. Berger, P. Schmuki, *Angewandte Chemie (International ed. in English)* **2011**, *50*, 2904.

[23] C. Humpel, *Neuroscience* **2015**, *305*, 86.

[24] S. G. Mayr, M. Moske, K. Samwer, *Phys. Rev. B* **1999**, *60*, 16950.

[25] H.-D. Hofmann, *BioValley Monogr.* **2005**, *1*, 58.

[26] E. R. Shamir, A. J. Ewald, *Nature reviews. Molecular cell biology* **2014**, *15*, 647.

[27] M. R. Lee, K. W. Kwon, H. Jung, H. N. Kim, K. Y. Suh, K. Kim, K.-S. Kim, *Biomaterials* **2010**, *31*, 4360.

[28] J. Xie, S. M. Willerth, X. Li, M. R. Macewan, A. Rader, S. E. Sakiyama-Elbert, Y. Xia, *Biomaterials* **2009**, *30*, 354.

[29] S. Oh, K. S. Brammer, Y. S. J. Li, D. Teng, A. J. Engler, S. Chien, S. Jin, *Proceedings of the National Academy of Sciences of the United States of America* **2009**, *106*, 2130.

[30] J. Padmanabhan, T. R. Kyriakides, *Wiley interdisciplinary reviews. Nanomedicine and nanobiotechnology* **2015**, *7*, 355.

[31] T. Igarashi, T. T. Huang, L. J. Noble, *Experimental Neurology* **2001**, *172*, 332.

[32] M. Davoli, J. Fourtounis, J. Tam, S. Xanthoudakis, D. Nicholson, G. Robertson, G. Ng, D. Xu, *Neuroscience* **2002**, *115*, 125.

[33] A. Weyer, K. Schilling, *Journal of neuroscience research* **2003**, *73*, 400.
[34] I. Unal-Cevik, M. Kilinc, Y. Gursoy-Ozdemir, G. Gurer, T. Dalkara, *Brain research* **2004**, *1015*, 169.
[35] L. T. McPhail, C. B. McBride, J. McGraw, J. D. Steeves, W. Tetzlaff, *Experimental Neurology* **2004**, *185*, 182.
[36] H. Kim, E. Kim, M. Park, E. Lee, K. Namkoong, *Progress in neuro-psychopharmacology & biological psychiatry* **2013**, *41*, 36.
[37] E. Wilhelmi, U. H. Schoder, A. Benabdallah, F. Sieg, J. Breder, K. G. Reymann, *Alternatives to laboratory animals ATLA* **2002**, *30*, 275.
[38] C. Humpel, *Frontiers in aging neuroscience* **2015**, *7*, 47.
[39] E. Balaur, J. M. Macak, H. Tsuchiya, P. Schmuki, *J. Mater. Chem.* **2005**, *15*, 4488.
[40] S. Mayazur Rahman, A. Reichenbach, M. Zink, S. G. Mayr, *Soft matter* **2016**, *12*, 3431.
[41] P. E. Scopelliti, A. Borgonovo, M. Indrieri, L. Giorgetti, G. Bongiorno, R. Carbone, A. Podesta, P. Milani, *PloS one* **2010**, *5*, e11862.
[42] Z. Lokmic, T. Lammermann, M. Sixt, S. Cardell, R. Hallmann, L. Sorokin, *Seminars in immunology* **2008**, *20*, 4.
[43] S. Vesentini, A. Redaelli, A. Gautieri, *Muscles, ligaments and tendons journal* **2013**, *3*, 23.
[44] R. Nitsch, I. Bechmann, R. A. Deisz, D. Haas, T. N. Lehmann, U. Wendling, F. Zipp, *Lancet (London, England)* **2000**, *356*, 827.
[45] J. Koerfer, S. Kallendrusch, F. Merz, C. Wittekind, C. Kubick, W. T. Kassahun, G. Schumacher, C. Moebius, N. Gassler, N. Schopow, D. Geister, V. Wiechmann, A. Weimann, C. Eckmann, A. Aigner, I. Bechmann, F. Lordick, *Cancer medicine* **2016**, *5*, 1444.
[46] C. A. Schneider, W. S. Rasband, K. W. Eliceiri, *Nature methods* **2012**, *9*, 671.

Figures

Figure 1

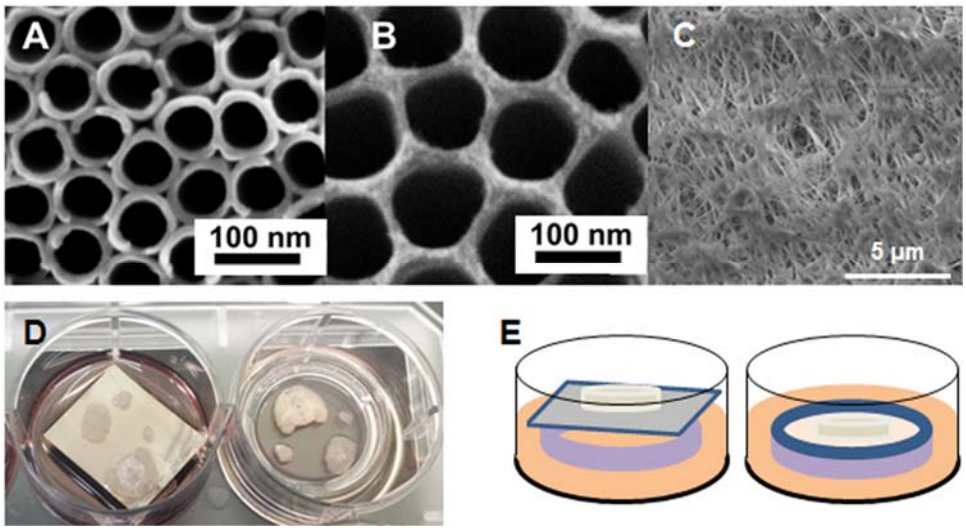

Figure 1. Surface structure of nanotube scaffolds and PTFE membranes and culturing scheme. (A, B) and (C) show SEM pictures of freestanding (FS) and nanoporous (NP) TiO_2 scaffolds and a PTFE membrane, respectively. (D) Tissue slices are cultivated at a liquid-air-interphase on a nanotube scaffold (left) and on a PTFE membrane insert (right) in a 6-well-plate. (E) Sketch of culture methods: For tissue culture on the ~ 100 µm thick nanotube scaffold, the scaffold – which appears like a usual metal plate – is placed on a few mm high ring as support material (left). Culture medium can be added under the scaffold into the 6-well-plate without covering the tissue with liquid. The medium flows from the side to the top of the nanotube surface. Right: Tissue culture on PTFE membranes.

Figure 2A

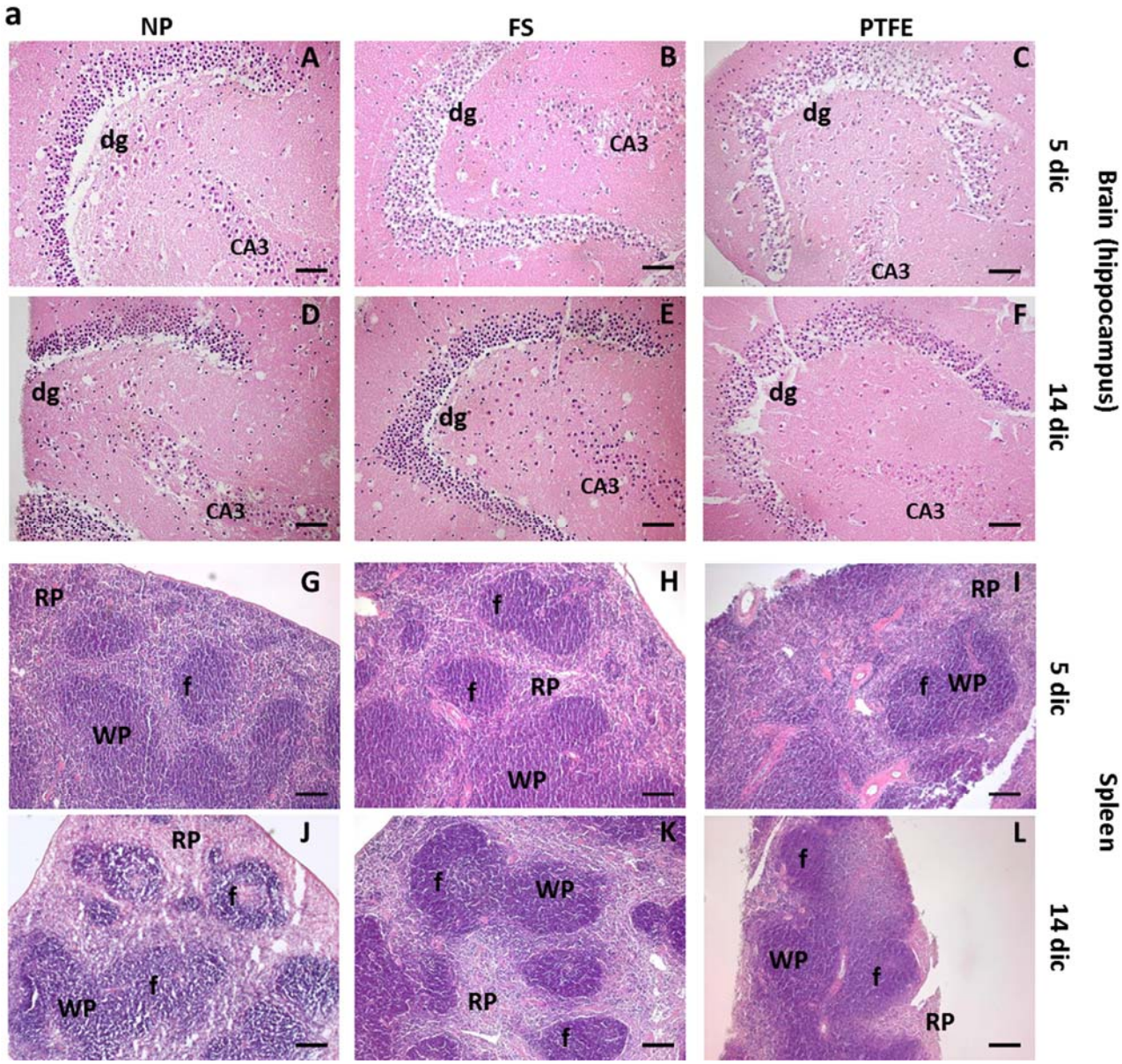
a
NP
FS
PTFE
A
B
C
dg
CA3
5 dic
D
E
F
14 dic
Brain (hippocampus)
G
H
I
RP
f
WP
5 dic
J
K
L
14 dic
Spleen

Figure 2B

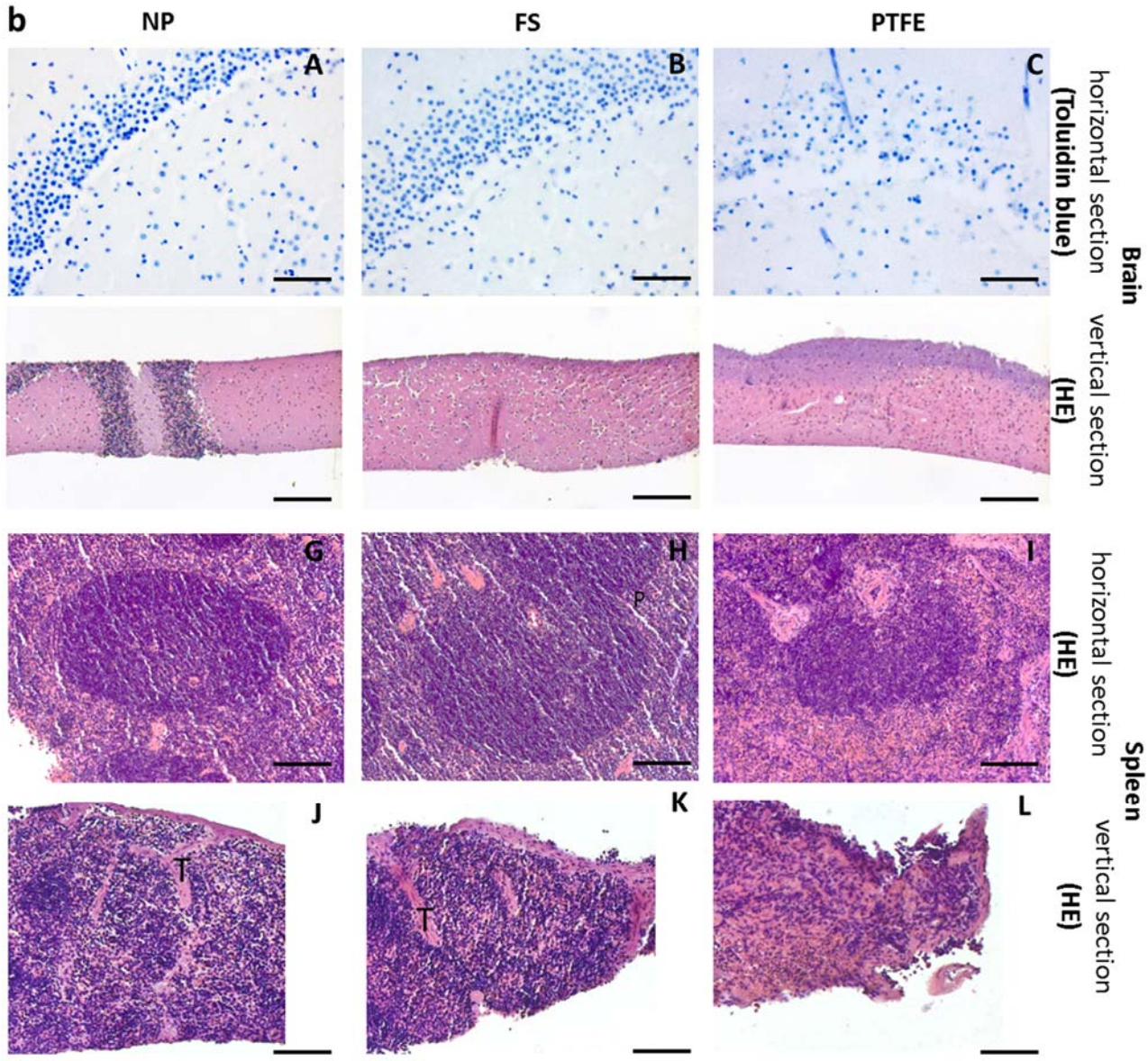

Figure 2. Morphological analysis of adult mouse brain and spleen tissue cultured on different materials. Brain and spleen tissue from adult wildtype C57 black 6 mice were cultured for 5 and 14 days on top of two different nanotube scaffolds (nanoporous, NP, left column; or freestanding, FS, middle column) and a PTFE filter membrane (right column). **2A:** HE staining of the hippocampal region in whole brain tissue slices after 5 dic **(A-C)** and 14 dic. Scale bar = 100 µm. **(D-F)**. For nanotube scaffolds, the morphology of the *dentate gyrus* (dg) is well preserved. Some condensed or fragmented nuclei of dying cells are present. Brain tissue cultured on PTFE membranes shows a clear degradation of structure

and neuronal cells in the *cornu ammonis* region 3 (CA3) as well as in the dg, however, to a minor extend. **(G-I)** HE-staining of spleen tissue slices after 5 dic and **(J-L)** 14 dic. Scale bar = 1 mm. The spleen morphology with follicles **(f)** and the surrounding capsule is better preserved on both nanotube types, in contrast to PTFE where the follicle structure and capsule integrity is widely dissolved at 5 dic **(I)**. **2B:** Brain and spleen cultures after 5 dic. Toluidine blue staining of DNA and endoplasmic reticulum shows good nucleus sustainment in the dg of brain tissue cultures grown on nanoporous scaffolds **(A)**. **(A-C)** Scale bar = 50 µm. Vertical examination of brain tissue cultures (HE) demonstrates a homogenous cellular distribution in tissue cultured on nanoporous scaffolds **(D)**. Brain tissue cultured on PTFE membranes, however, showed a clear gradient and an enhanced acidic tissue layer towards the surface of the culture **(F)**. Follicle cells migrate and connective tissue proliferates in spleen cultures on PTFE membranes **(I)**, which is not observed in spleen tissue cultured on nanotube scaffolds **(G, H)**. Vertical examination of spleen tissue cultures (HE) shows that spleen architecture and capsular integrity is best maintained on FS scaffolds **(K)**, whereas spleen tissue of PTFE membranes loses its architecture completely **(L)**; spleen tissue of nanotube scaffolds shows a denser capsule **(J)**. **(D-L)** Scale bar= 200µm. RP = red pulp. WP = White Pulp. T = trabecula.

Figure 3

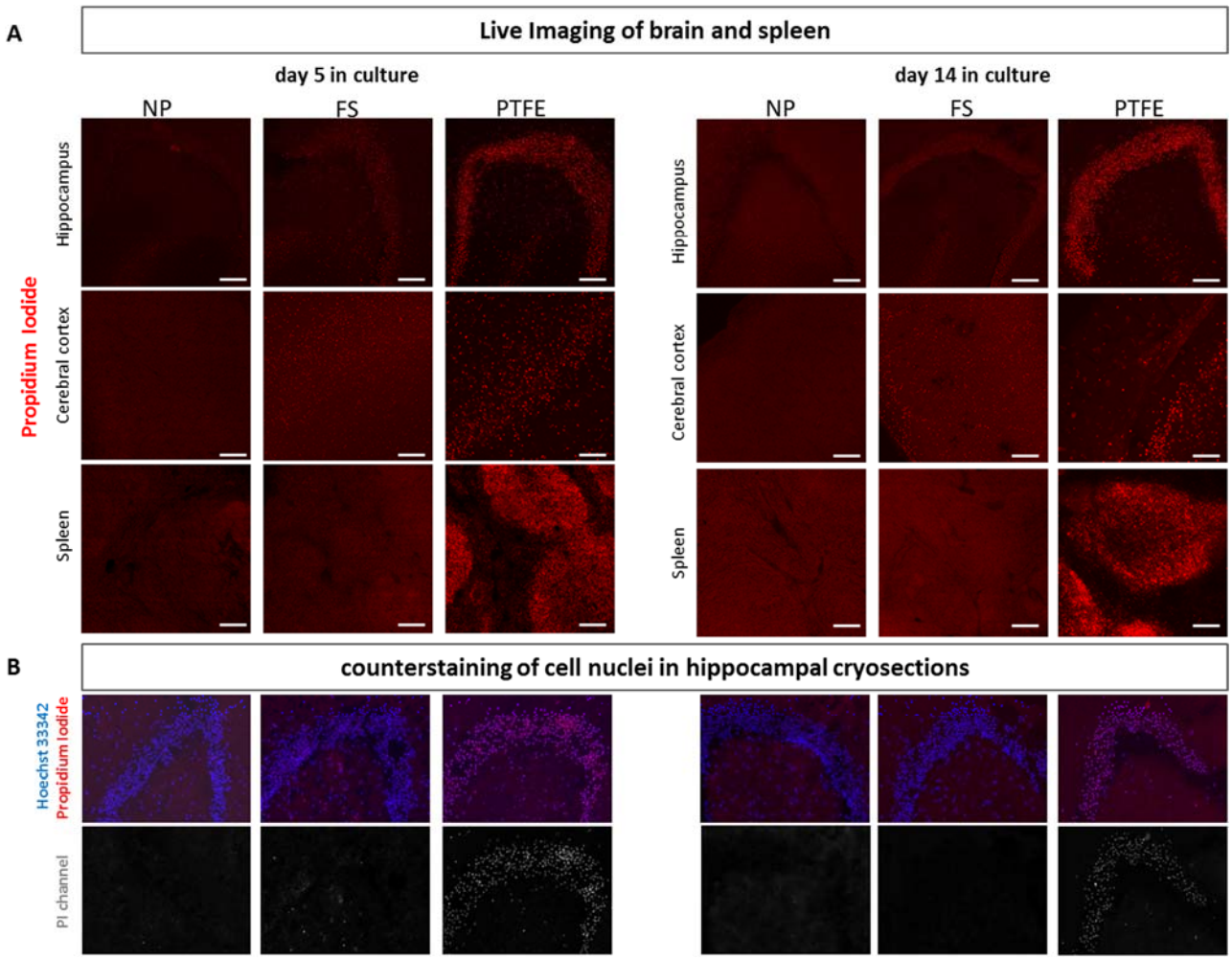

Figure 3. Live imaging of adult brain and spleen tissue cultured on nanotube scaffolds and PTFE membrane. Brain and spleen of adult wildtype C57/BL6 mice were cultivated for 5 (A) and 14 (B) days on two different nanotube scaffolds (nanoporous, NP, left row in A and B, and freestanding, FS, middle row in A and B), as well as standard PTFE membrane inserts (right row in A and B). **(A)** After 5 dic brain tissue cultured on PTFE membrane shows high contents of PI positive cells in the hippocampal as in cortical regions in contrast to brain tissue cultured on NP scaffolds. Brain tissue cultured on FS scaffolds also reveals several PI positive nuclei in both investigated regions. The same outcome was obtained after 14 dic. Spleen tissue cultures were best maintained on FS scaffolds, as less PI positive nuclei were observed after 14 dic compared with NP scaffolds. PTFE membranes could not preserve

spleen tissue in culture as almost all nuclei were PI positive. **(B)** Brain tissue was fixated after 5 and 14 dic and counterstained with Hoechst 33342. PI uptake was increased at both timepoints in all tissue cultures cultivated on PTFE. Here, the hippocampal region with the *dentate gyrus* region is shown (A) and (B) Scale bar: 200 µm; N=3.

Figure 4

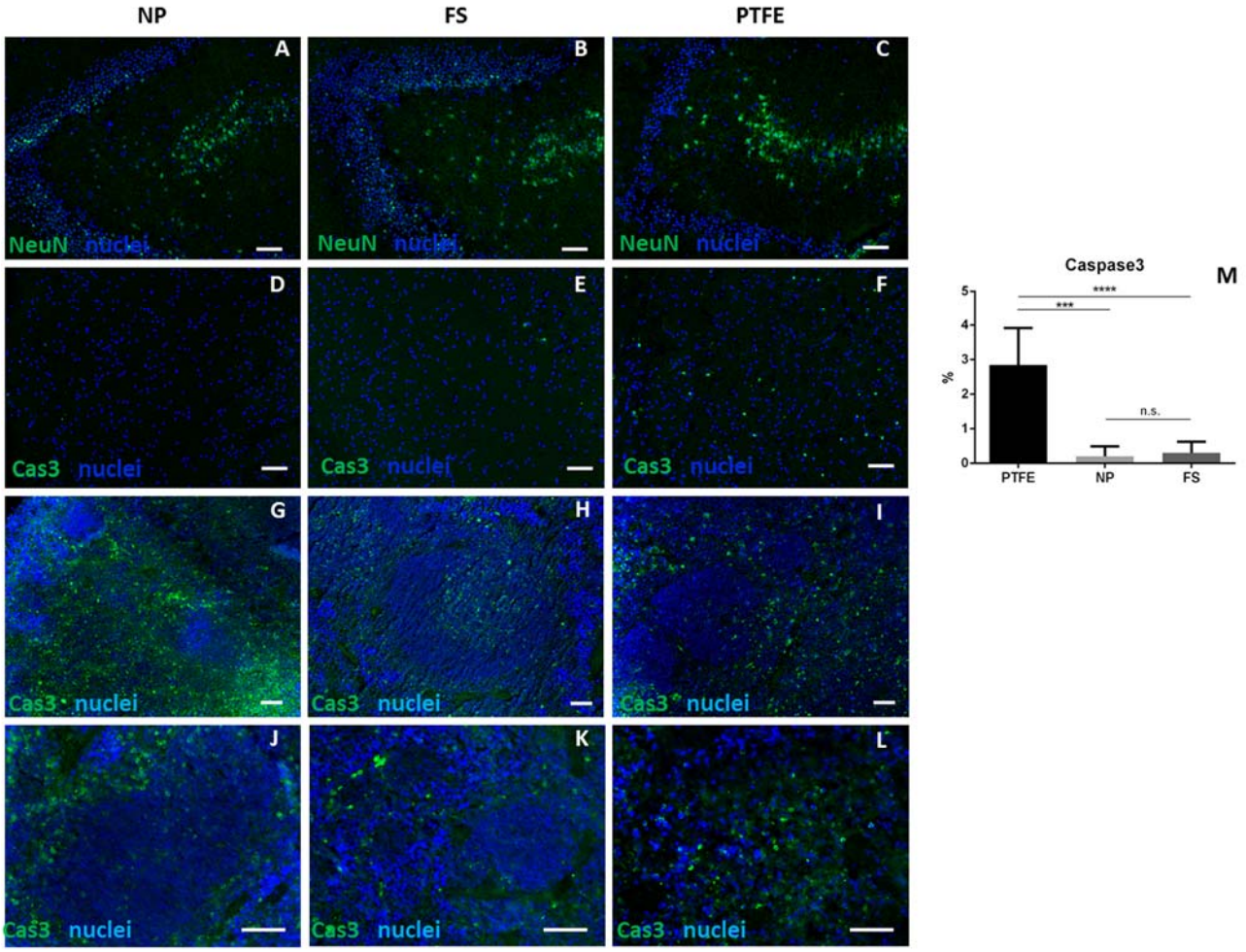

Figure 4. Immunohistocemical analysis of mouse brain and spleen tissue cultured on different scaffolds. Brain and spleen tissue from adult wildtype C57 black 6 mice was cultured for 5 days on top of two different nanotube scaffolds (nanoporous, NP, left column; freestanding, FS, middle column) and a PTFE filter membrane (right column). **(A-C)** Visualization of neurons (NeuN, green) and nuclei (Hoechst 33342, blue) in the hippocampal region of brain slices. **(D-F)** Immunocytochemical staining for the apoptosis marker cleaved Caspase 3 (green) and nuclear counterstain (blue) on horizontal cryosections of brain slices (cortex). Apoptotic cells are almost absent in tissue of NP nanotube scaffolds **(D)**, and only very few occur in tissue on FS scaffolds **(E)**, while a large number of apoptotic cells appears in tissue on PTFE membranes **(F)**. **(G-L)** Immunocytochemical staining for the apoptosis marker cleaved Caspase 3 (green) and nuclear counterstain (blue) on horizontal

cryosections of spleen slices. Here, several apoptotic cells became visible on all culture scaffolds and were therefore not further quantified due to irregular tissue morphology. **(M)** Apoptotic fraction of cells in brain slice cultures (5 dic) was determined by relating Caspase 3 positive cells to total cell number. All scale bars represent 500 µm.

Figure 5

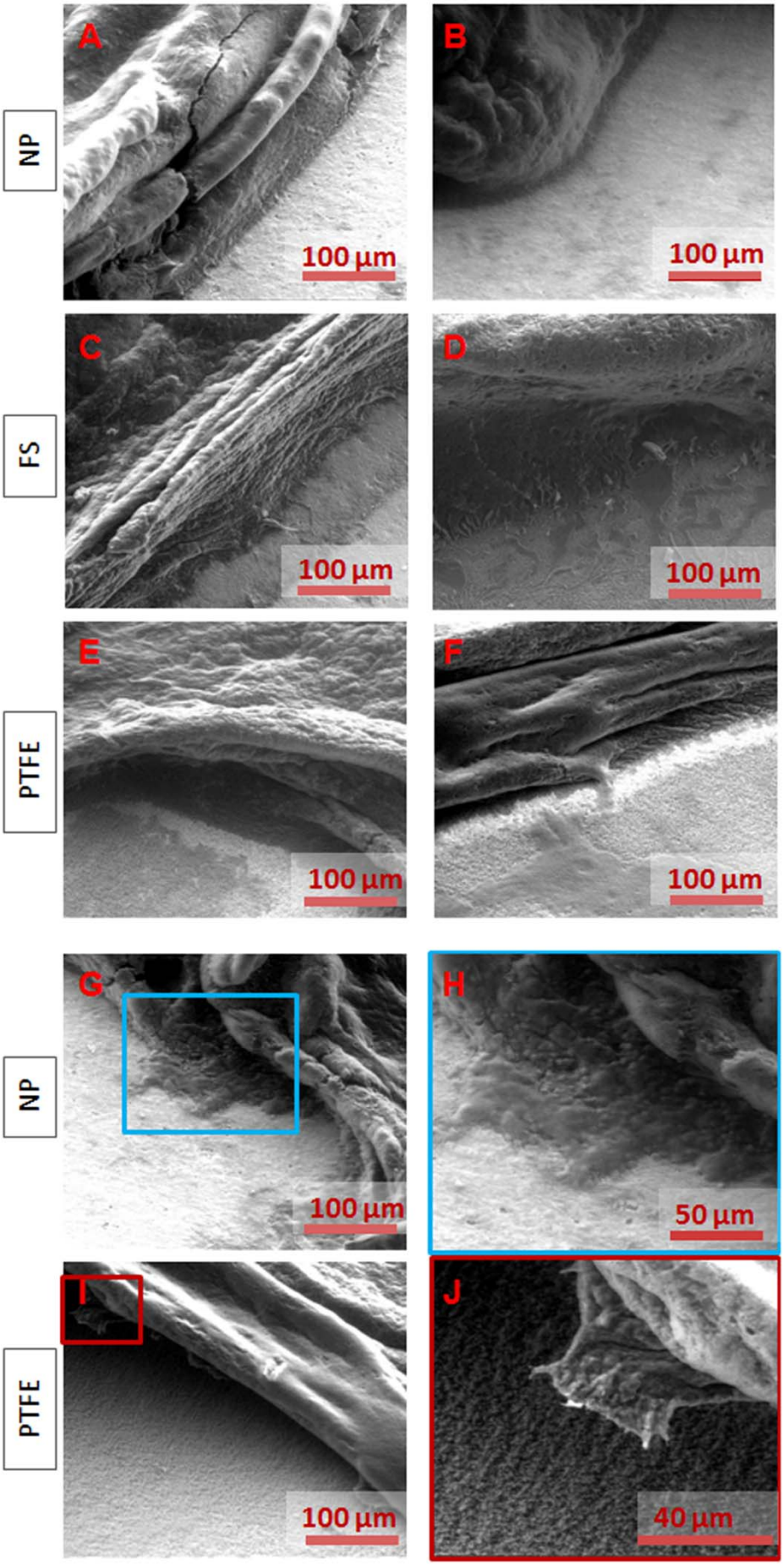
NP
A
100 µm
B
100 µm
FS
C
100 µm
D
100 µm
PTFE
E
100 µm
F
100 µm
NP
G
100 µm
H
50 µm
PTFE
I
100 µm
J
40 µm

Figure 5. Environmental scanning electron microscopy images of adult mouse brain tissue slices after 5 dic on different scaffolds. **(A-B)** Tissue on nanoporous (NP) nanotube scaffolds with a diameter of 57.6±1.2 nm and **(C-D)** freestanding (FS) nanotubes with a diameter of 100.0±12.0 nm; **(E-F)**: Tissue cultured on a PTFE membrane with an average pore diameter of 0.4 µm (Millipore). While for the nanotube scaffolds, the tissue adhered to the scaffold along the entire tissue-scaffold intersection (B and D), on PTFE membranes only single adhesion spots are visible (F). Another example for a continuous adhesive border between the tissue and the NP nanotube scaffold is shown in **(G)** and the magnification (blue box) in **(H)**. In contrast, adhesive spots between the tissue and the PTFE membrane **(I)** is magnified with a red box in **(J)**.